

Effect of mechanical load on the shuttling operation of molecular muscles

Seungjun Lee and Wei Lu^{a)}*Department of Mechanical Engineering, University of Michigan, Ann Arbor, Michigan 48109, USA*

(Received 30 April 2009; accepted 22 May 2009; published online 10 June 2009)

We use molecular dynamics simulations to investigate the effect of mechanical force on stimulus-induced deformation of rotaxane-based artificial molecular muscles. The study shows that a small external force slows down the shuttling motion and leads to longer actuation time for a muscle to reach its full extension. Further increase in the force can significantly reduce the traveling distance of the ring, leading to reduced strain output. A force larger than 28 pN can completely suppress the shuttling motion, suggesting a limit of force output of molecular muscles. © 2009 American Institute of Physics. [DOI: 10.1063/1.3153509]

Artificial molecular muscles have recently attracted considerable interest. A particularly notable system is bistable rotaxanes, which are composed of mutually recognizable ring and dumbbell-shaped components.^{1,2} Upon the application of an external stimulus, which can be chemical, electricity, or light, the ring component can be switched back and forth between the two recognition sites along the dumbbell-shaped component, thereby enabling rotaxanes to behave like molecular muscles. These molecular-scale systems utilize a “bottom-up” technology centered around the design and manipulation of molecular assemblies, and are potentially capable of delivering efficient actuations at dramatically reduced length scales when compared to traditional microscale actuators. These molecular muscles can be integrated with microelectromechanical/nanoelectromechanical systems technology to produce nanoscale machines or devices, such as logical switches between metallic electrodes³ and mechanical actuators.⁴ When these molecular muscles are coated on top of microcantilevers, consecutive oxidation and reduction can drive the microbeams for repeated bending and restoring.^{5,6}

When employed for functional nanodevice applications, the molecular muscles are connected to external constraints such as substrates or other load-bearing components. It is thus important to understand how external loading affects the ring switching process, which is central to the actuation function. Take beam deflection as an example. Depending on the density of the molecular muscles on the beam surface, the force that a molecular muscle has to generate would be different. If the density is low, the mechanical load that a molecular muscle needs to carry can be too high so that the device will not function properly. If the relation between the mechanical load and the work output of a molecular muscle is understood, the number, location, and density of molecular muscles for the required bulk output can be optimized. Thus, development of advanced engineering applications requires fundamental understanding of molecular muscles under stressed state. How much force can a molecular muscle generate? What is the relation between stimulus-induced strain and the constraint of external force? In this letter we employ molecular dynamics simulations to systematically address these issues.

Figure 1 shows the model we have studied, which is a daisy-chain molecular muscle composed of two linear bistable [2]rotaxanes mechanically interlocked with each other. Each side of the bistable [2]rotaxane has two recognition sites of tetrathiafulvalene (TTF) and hydroquinone (HQ). The ring component is cyclobis(paraquat-p-phenylene) (CBPQT⁴⁺). When the TTF site is charged due to external stimulus, the ring switches to the other site due to the electrostatic repulsion between the ring and the oxidized station.

We use DREIDING force field and LAMMPS software for molecular dynamics calculations. DREIDING force field has been well tested for organic molecules including bistable rotaxanes.⁷ The total potential energy of an arbitrary geometry of a molecule is expressed as a superposition of valence interactions that depend on the specific connections of the structure, and nonbonded interactions that depend only on the distance between the atoms. The valence interactions consist of bond stretch, bond-angle bend, dihedral angle torsion, and inversion terms, while the nonbonded interactions consist of van der Waals interaction and electrostatic interaction. The parameters for the force fields and the pair interactions between heterogeneous atoms follow those published data.⁸ The simulations are performed using the canonical en-

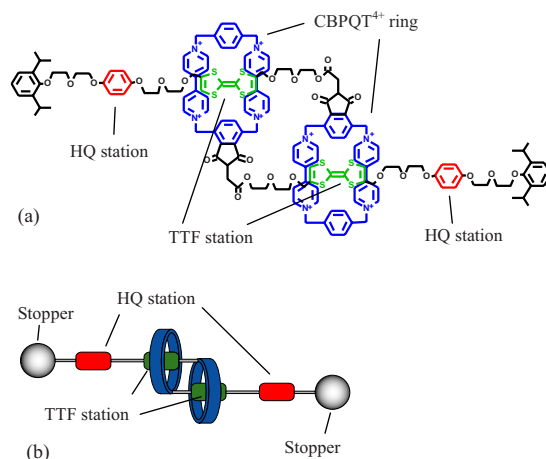


FIG. 1. (Color online) (a) Structural formula of the daisy-chain artificial molecular muscle composed of two linear bistable [2]rotaxanes mechanically interlocked with each other. Each side of the bistable rotaxane has two recognition sites of TTF and HQ. The ring component is (CBPQT⁴⁺). (b) Schematic representation of the model.

^{a)}Author to whom correspondence should be addressed. Electronic mail: weilu@umich.edu.

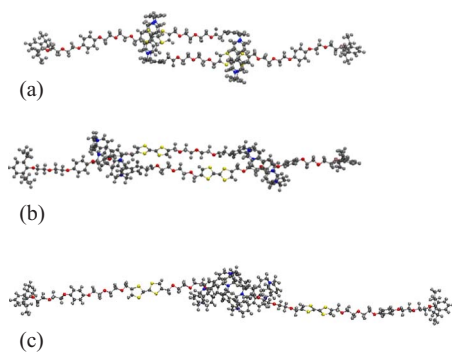


FIG. 2. (Color online) Representative results of molecular dynamics simulations. (a) Initial configuration for all simulations. (b) Snapshot of the structure at $t=10$ ps under an applied force of 21 pN. The rings move away from each other due to electrostatic repulsion between the oxidized TTF station and the ring. (c) Snapshot of the structure at $t=10$ ps under an applied force of 30 pN. The rings are pulled closer since the applied force is larger than the electrostatic repulsion.

semble (*NVT*) with Nose–Hoover thermostat^{9,10} with the relaxation time of 0.1 ps. The temperature is set to 300 K. The Verlet algorithm¹¹ is used to integrate the equation of motion. A time step of 1 fs is used and each simulation is calculated up to 10 ps, which is enough to observe the influence of the external forces.

The partial atomic charges used in the electrostatic energy term are calculated by quantum mechanics using GAUSSIAN software.¹² The total charge of the oxidized structure is +12 electron charges, two ring components each originally charged with +4 electron charges and two TTF stations each charged with +2 electron charges. When the partial atomic charges are calculated, the molecular structure is decomposed into ring, TTF unit, HQ unit, and chains connecting these pieces. The total charges are set to neutral except the ring and the TTF units in the quantum mechanics calculation. Although this approach may not give the exact distribution of atomic charges, it is reasonable in this simulation since we focus on the ring switching as an entire piece. All the quantum mechanics calculations use B3LYP of density functional theory with 6–31G basis set.

To investigate the effect of external forces, we add extra force to one of the hydrogen atoms at the stoppers that are located at the end of the molecular structure. The forces are varied from 1 to 30 pN with an increment of 1 pN. Figure 2 shows representative results for molecular dynamic simulations. We measure the relative distance between the two ring components in each simulation. Figure 3 shows representative results for relatively small external forces. The horizontal axis shows the time step while the vertical axis shows the relative distance between two rings. The zero in the vertical axis refers to the initial distance between two rings when they are located at the TTF stations. A positive value is defined as the increase in the ring distance, which is directly related to the contraction of the muscle as shown in the inset. It is found that the first peak of separation appears at about the time step of 2 ps. The appearance of the first peak is gradually delayed with the increase in the external force. This is reasonable since the external forces act opposite to the ring movement direction. A larger force slows down the ring movement more.

The distance curves show a wavy shape. The repulsion between the ring and oxidized TTF station drives the rings to

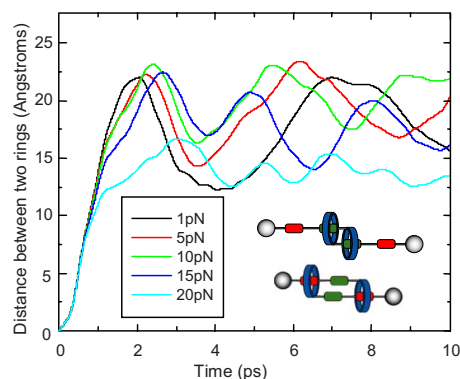


FIG. 3. (Color online) The relative distance between two rings under various applied forces in the range of less than 20 pN. The zero in the vertical axis refers to the initial distance between two rings when they are located at the TTF stations. A positive value is defined as the increase in the ring distance, which is directly related to the contraction of the muscle as shown in the inset.

separate from each other and each move toward the corresponding HQ station. In addition to this major interaction, the ring-ring repulsion helps the separation while the repulsion between the two charged TTF stations retards the action. The conversion between kinetic and potential energy causes the ring to vibrate. The mean distance is a good indication of the ring separation change. As the external force increases, the period and amplitude of the vibration decreases. Thus, if we consider the structure as a vibrating ring-spring system, the external force essentially makes the spring stiffer.

When the applied force is relatively large, the distance curve shows significant decrease in the mean distance by moving downward. The 20 pN curve in Fig. 3 shows this trend with a mean relative distance of about 14 Å. In this case the ring finds an equilibrium position determined by the external force and the electrostatic repulsion together. Figure 4 shows the curves under external forces between 21 and 30 pN. When the applied force is over 20 pN, the mean relative distance between the rings reduces to less than 14 Å. A force larger than 28 pN can even reduce the distance between rings to less than the original separation. In somewhere between 27 and 28 pN, the external force can hold the rings at the original equilibrium positions when the external force just balances the repulsion. The reason that the curve of 26 pN shows depression between two humps around the time step of 1.5 ps is that the ring temporarily gets stuck as it is tilted

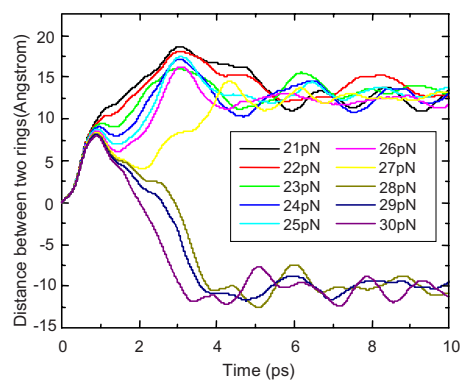


FIG. 4. (Color online) The relative distance between two rings under forces in the range between 21 and 30 pN. A force larger than 28 pN can completely suppress the strain generation.

by the large force transmitted to one side of the ring structure. In contrast, with an applied force of 21 pN the ring moves smoothly to the maximum position because the force is not large enough to make the ring tilt.

When the external force is over 28 pN the graph shows a sudden change in the shape and ends up with negative values. This means the two rings come closer. In this range of external forces the electrostatic repulsion cannot provide enough driving force to push the rings. Therefore, the ring structures are pulled together by the external forces. At this stage the molecular muscle cannot produce any contraction strain and loses its capability as actuators. Note that the effect of the external force does not occur immediately when the simulation is started. Thus, the two rings still separate from each other at the beginning, which corresponds to the positive segments in the curve. After about 1 ps the force is transmitted to the ring and starts to pull it to the direction of the force. Then quickly the two rings move toward each other and the curves become negative.

In summary, the study reveals the operation of artificial molecular muscles composed of two rotaxanes. Increasing external force leads to longer actuation time and smaller achievable strain. A large force can completely suppress the strain generation. Simulations show that the muscle can generate a maximum force output of 28 pN, beyond which no contraction strain can be achieved. The results can be useful

for the prediction of the performance and design of nanomachines assembled with molecular muscles.

The authors acknowledge financial support from National Science Foundation CAREER Grant No. DMI-0348375.

- ¹R. A. Bissell, E. Cordova, A. E. Kaifer, and J. F. Stoddart, *Nature (London)* **369**, 133 (1994).
- ²J. P. Sauvage, *Science* **291**, 2105 (2001).
- ³C. P. Collier, E. W. Wong, M. Belohradsky, F. M. Raymo, J. F. Stoddart, P. J. Kuekes, R. S. Williams, and J. R. Heath, *Science* **285**, 391 (1999).
- ⁴B. K. Juluri, A. S. Kumar, Y. Liu, T. Ye, Y. W. Yang, A. H. Flood, L. Fang, J. F. Stoddart, P. S. Weiss, and T. J. Huang, *ACS Nano* **3**, 291 (2009).
- ⁵T. J. Huang, B. Brough, C. M. Ho, Y. Liu, A. H. Flood, P. A. Bonvallet, H. R. Tseng, J. F. Stoddart, M. Baller, and S. Magonov, *Appl. Phys. Lett.* **85**, 5391 (2004).
- ⁶Y. Liu, A. H. Flood, P. A. Bonvallet, S. A. Vignon, B. H. Northrop, H. R. Tseng, J. O. Jeppesen, T. J. Huang, B. Brough, M. Baller, S. Magonov, S. D. Solares, W. A. Goddard, C. M. Ho, and J. F. Stoddart, *J. Am. Chem. Soc.* **127**, 9745 (2005).
- ⁷S. S. Jang, Y. H. Jang, Y. H. Kim, W. A. Goddard, J. W. Choi, J. R. Heath, B. W. Laursen, A. H. Flood, J. F. Stoddart, K. Norgaard, and T. Bjornholm, *J. Am. Chem. Soc.* **127**, 14804 (2005).
- ⁸S. L. Mayo, B. D. Olafson, and W. A. Goddard III, *J. Phys. Chem.* **94**, 8897 (1990).
- ⁹W. G. Hoover, *Phys. Rev. A* **31**, 1695 (1985).
- ¹⁰S. Nose, *J. Chem. Phys.* **81**, 511 (1984).
- ¹¹L. Verlet, *Phys. Rev.* **159**, 98 (1967).
- ¹²www.gaussian.com